

1 **Dietary iron interacts with diet composition to modulate the endocannabinoidome and the**
2 **gut microbiome in mice**

3 **Fredy Alexander Guevara Agudelo^{1,2,3}, Nadine Leblanc^{1,2}, Isabelle Bourdeau-Julien^{1,2,3}, Gabrielle**
4 **St-Arnaud^{1,2,3}, Fadil Dahhani^{2,4}, Nicolas Flamand^{2,4}, Alain Veilleux^{1,2,3}, Vincenzo Di Marzo^{1,2,3,4},**
5 **Frédéric Raymond^{1,2,3*}**

6
7 ¹ Centre Nutrition, santé et société (NUTRISS), et Institut sur la Nutrition et les aliments fonctionnels
8 (INAF), Université Laval, Québec, Canada.

9 ² Chaire d'excellence en recherche du Canada sur l'axe microbiome - endocannabinoidome dans la santé
10 métabolique (CERC-MEND).

11 ³ École de nutrition, Faculté d'agriculture et des sciences de l'alimentation, Université Laval, Québec,
12 Canada.

13 ⁴ Faculté de médecine, Institut universitaire de cardiologie et pneumologie de Québec, Université Laval,
14 Québec, Canada.

15
16 *E-mail: frederic.raymond@fsaa.ulaval.ca

17 **Author contributions**

18 Conceptualization, F.A.G.A., N.L., V.D., and F.R.; Methodology, F.A.G.A., N.L., G.S., and F.R.; Formal
19 Analysis, F.A.G.A., I.B.J., N.F., N.F., V.D., and F.R.; Data Curation, F.A.G.A and F.R.; Writing—
20 Original Draft, F.A.G.A, V.D, and F.R.; Writing—Review and Editing, F.A.G.A., I.B.J., N.F., G.S., N.F.,
21 A.V., V.D., and F.R.; Supervision, V.D. and F.R; Funding Acquisition, V.D., and F.R.

22



CAMBRIDGE
UNIVERSITY PRESS

This peer-reviewed article has been accepted for publication in Gut Microbiome but has not yet been copy-edited or typeset so may be subject to change during the production process. The article is considered published and may be cited using its DOI:

10.1017/gmb.2025.1

Gut Microbiome is co-published by Cambridge University Press and The Nutrition Society.

This is an Open Access article, distributed under the terms of the Creative Commons Attribution-NonCommercial-NoDerivatives licence (<http://creativecommons.org/licenses/by-nc-nd/4.0/>), which permits non-commercial re-use, distribution, and reproduction in any medium, provided the original work is unaltered and is properly cited. The written permission of Cambridge University Press must be obtained for commercial re-use or in order to create a derivative work.

23 **Abstract:**

24 The endocannabinoidome (eCBome) and the gut microbiota have been implicated in diet-induced obesity
25 and impaired metabolism. While the eCBome and the gut microbiome are known to respond to diet
26 macronutrient composition, interaction with micronutrient intake has been relatively unexplored. Iron (Fe)
27 is an essential micronutrient for the function of enzymes involved in energy and lipid metabolism. Here,
28 we evaluated how 28 days of Fe depletion and enrichment, in interaction with Low Fat-Low Sucrose
29 (LFLS) or High Fat-High Sucrose (HFHS) diets, affect the host via the eCBome, and modulate intestinal
30 gut microbial communities. Circulating levels of *N*-oleoyl-ethanolamine (OEA) showed an elevation
31 associated with Fe-enriched LFLS diet, while the Fe-depleted HFHS diet showed an elevation of *N*-
32 arachidonoyl-ethanolamine (anandamide, AEA) and a decrease of circulating linoleic acid. In parallel, the
33 response of intestinal inflammatory mediators to Fe in the diet showed decreased levels of prostaglandins
34 PGE₁, PGE₃ and 1a,1b-dihomo PGF₂α in the caecum. Individual differences in microbial taxa were less
35 pronounced in the ileum than in the caecum, where *Eubacterium coprostanoligenes* group showed an
36 increase in relative abundance associated with Fe-depleted LFLS diets. In conclusion, our study shows that
37 Fe intake modulates the response to the macronutrient composition of the diet in mice.

38 **Keywords:** Microbiome, iron, endocannabinoid (eCB) system, nutrition, inflammation, metabolic health,
39 intestine.

40 Introduction

41 Iron (Fe) is a fundamental micronutrient that plays a role in oxygen transport (Lakhal-Littleton & Robbins,
42 2017), the synthesis of metabolic enzymes (Cerami, 2017), cellular respiration (Oexle et al., 1999), and the
43 maintenance of normal immune function (Ni et al., 2022). Fe mediates electron transfer and oxygen supply
44 in oxidation-reduction reactions which, although vital for maintaining normal cellular metabolism, can also
45 result in the generation of toxic reactive oxygen species ROS (Hentze et al., 2004). Fe is obtained from the
46 diet in different forms and can be classified into two types: heme-Fe and non-heme Fe. Heme-Fe is found
47 mainly in animal products and is the most bioavailable form, with absorption rates between 15% and 35%.
48 This form of Fe is readily absorbed, but accounts for only 5-10% in most diets.

49 Obesity is associated with low-grade chronic inflammation (Ellulu et al., 2017) and, over the last
50 few years, it has been reported that this condition alters Fe metabolism. In adults and children, obesity is
51 linked to hypoferrremia, impaired Fe absorption and lower Fe stores despite adequate dietary Fe intake
52 (Baumgartner et al., 2013). In particular, individuals with obesity or combined chronic inflammatory
53 diseases are more likely to have hypoferrremia, which could be associated to Fe deprivation caused by the
54 inflammatory response (Yanoff et al., 2007). Reduced plasma ferritin has been previously observed to
55 improve nonalcoholic fatty liver disease in individuals with obesity, suggesting that it is essential to
56 consider the Fe status in the treatment of obesity-related metabolic dysfunction (Moore Heslin et al., 2021).
57 Recent studies have emphasized the importance of Fe in the regulation of lipid homeostasis (Rodríguez-
58 Pérez et al., 2018). Indeed, both Fe insufficiency, especially in severe obesity (Aigner et al., 2014) and Fe
59 overload syndrome has been well studied in association with obesity-related diseases (Moore Heslin et al.,
60 2021).

61 Host-microbiota interactions are directly influenced by Fe, which alters bacterial growth in the
62 intestine. Both deficiency and excess of Fe are important in terms of gut microbiota dysbiosis. Dysbiosis
63 has been associated with a number of human diseases, such as autoimmune disorders (Collado et al., 2015),
64 increased vulnerability to cancers (Viaud et al., 2014), irritable bowel syndrome (Kostic et al., 2014), and
65 the progression of obesity (Boulangé et al., 2016). Gut microbiota and their metabolites could potentially
66 exert an influence on inflammatory conditions in the host (Feng et al., 2018). Indeed, it is well known that
67 gut microbiota plays a major role in the development of food absorption and low-grade inflammation (Al
68 Bander et al., 2020). Although there are increased amounts of dietary Fe in the colon, bacteria may still
69 compete to incorporate Fe due to the formation of Fe complexes with other food components and the low
70 solubility of ferric Fe due to a higher pH in the colon (Kortman et al., 2014). Immune-mediated
71 inflammatory diseases, such as Crohn's disease (CD), ulcerative colitis (UC), multiple sclerosis (MS), and

72 rheumatoid arthritis (RA), modify the composition of the gut microbiota and Fe has also been linked to the
73 development of these diseases (Kaitha et al., 2015).

74 Fe is an essential cofactor for peroxidase, lipoxygenase and cyclooxygenase enzymes involved in
75 the catabolism of arachidonic acid. Arachidonic acid (AA) plays essential roles, especially in cell signalling
76 through its role as a precursor of numerous eicosanoids such as prostaglandins and leukotrienes. Indeed,
77 previous studies have shown that Fe-citrate but not sodium citrate (Na-citrate) downregulates the production
78 of PGE₂ (Hisakawa et al., 1998). Moreover, AA is also a molecular block of the endocannabinoids 2-
79 arachidonoyl-glycerol (2-AG) and *N*-arachidonoyl-ethanolamine (Anandamide or AEA), that have
80 signalling functions in appetite regulation and energy metabolism, in relation to the modulation of
81 neurotransmitter release (Almeida et al., 2022), which could involve physiological and pathophysiological
82 phenomena.

83 The endocannabinoid system (eCBs) is a signalling system comprised of endogenous lipids
84 mediators, the endocannabinoids AEA (also known as anandamide) and 2-AG, which bind to two G protein-
85 coupled receptors, the cannabinoid type 1 and type 2 (CB₁ and CB₂) receptors, expressed throughout the
86 body. The endocannabinoidome (eCBome) is defined as an extension of the eCBs that also includes the
87 congeners of AEA and 2-AG, the *N*-acyl-ethanolamines (NAEs) and 2-monoacyl-glycerols (2-MAGs),
88 respectively, together with additional enzymes and receptors related to these molecules (Iannotti & Di
89 Marzo, 2021). Endocannabinoids and their congeners are synthesized from membrane phospholipid
90 precursors containing the corresponding fatty acids either esterified to the 2-hydroxy group of glycerol in,
91 usually, phosphatidylinositol, for 2-MAGs, or amidated by the NH₂-group of phosphatidylethanolamine,
92 for NAEs (Simard et al., 2022). The eCBome is involved in several physiological processes such as satiety,
93 energy control and other essential functions in metabolic health (Silvestri & Di Marzo, 2013). For instance,
94 *N*-oleoyl-ethanolamine (OEA) can inhibit food intake, while palmitoylethanolamide (PEA) has anti-
95 inflammatory activity through the activation of several receptors including peroxisome proliferator-
96 activated receptor α (PPAR α) (Alhouayek & Muccioli, 2014). The eCBome mediates a number of
97 physiological and pathophysiological responses in the intestine via activation of the cannabinoid receptors,
98 TRPV channels and several GPR, for example maintaining homeostasis in the gut by controlling
99 hypercontractility and permeability, and promoting regeneration after injury (Taschler et al., 2017). The
100 small intestine serves both as an organ for digestion and absorption of food, and for signaling to the brain
101 and peripheral organs about the amount of incoming food (Psichas et al., 2015). NAEs and 2-MAGs may
102 participate in the regulation of gut-brain signalling in relation to the control of food intake.

103 The crosstalk between the intestinal eCBome and gut microbiota regulates many gastrointestinal
104 functions, such as hormone secretion, intestinal permeability, motility, immune response and nutrient
105 absorption (Cuddihey et al., 2022). There are numerous environmental and host genetic factors which can

106 impact on the structure of the intestinal microbiota, but diet is considered to be a main driver (Moles &
107 Otaegui, 2020). Studies have been focused on exploring the impact of macronutrients, such as
108 carbohydrates and proteins, on colonic and fecal bacterial populations (Castonguay-paradis et al., 2020;
109 Rowland et al., 2018). However, there have been substantially fewer investigations on the modulatory
110 effects of micronutrients. Previous studies have demonstrated that lipid mediators, including the eCBome,
111 can be modulated by micronutrients in interaction with the macronutrient composition of the diet (Guevara
112 Agudelo et al., 2022).

113 In this work, we investigated how diets depleted (12 mg/kg) or enriched (150 mg/kg) in Fe
114 modulate the eCBome and gut microbiome response to a Low Fat-Low Sucrose (LFLS) or High Fat-High
115 Sucrose (HFHS) diet in an obesity mice model. Intake of Fe was chosen to represent low and high Fe
116 consumption without inducing deficiency nor toxicity, thus covering the full range of safe dietary intake
117 (Asperti et al., 2018; B R Blakley, 1988; Nutrition, 1995). Our hypothesis is that the host response to diet
118 macronutrient composition will be affected by Fe intake. Specifically, we studied the response of the
119 circulating eCBome, as well as the ileum and caecum eCBome, microbiome and inflammation mediators.
120 Special attention is given to the intestinal response to dietary conditions, as the intestine is the first organ
121 to be exposed to the diet. Experiments were conducted with male and female mice to examine the impact
122 of Fe and diet formulation on gut microbiota and eCBome. The data were then stratified to assess the
123 influence of sex on the responses of mice to Fe. Our results highlight the complexity of studying dietary
124 components, as many interactions were observed between Fe intake and diet macronutrient composition.

125

126 **Materials and methods:**

127 **Animals, diets, and housing**

128 The study was approved by the Université Laval animal ethics committee (CPAUL 2019-006). Forty-eight
129 6-week-old C57BL/6J male and female mice were purchased from Jackson Laboratory (USA) and were
130 individually housed in the animal facility of the Institute of Nutrition and Functional Foods (INAF), in
131 standard cages under controlled temperature (22°C) and relative humidity (50%) with a 12 h day/night
132 cycle. At arrival, all mice were acclimated to their new environment for a one-week adaptation period,
133 during which they received a normal chow diet (AIN-93G-purified diet #110700, Dyets Inc., Bethlehem,
134 PA, USA). Following this time, mice were randomly assigned to 4 groups (n=12 per group, 6 males and 6
135 females). The groups were defined according to 4 diet designs. Table S1 presents the formulation for the
136 four diet groups set as follows: Enriched (150 mg/kg) and depleted (12 mg/kg) concentrations of Fe in
137 combination with High Fat-High Sucrose (HFHS: 23.6% fat, 17% sucrose, Research Diets Inc., NJ, USA),
138 and Low Fat-Low Sucrose (LFLS: 4.3% fat, 7% sucrose, Research Diets Inc., NJ, USA). In this study, Fe
139 was provided as ferric citrate. The diets were formulated to be isonitrogenous, although different in energy

140 and lipid content between HFHS and LFLS. Total energy in diets was determined with an adiabatic Parr
141 6300 calorimeter (Parr Instrument Company, Moline, IL, USA) and was similar among LFLS and among
142 HFHS diets (Fe-depleted LFLS 3967.15 cal/g; Fe-enriched LFLS 3906.3 cal/g; Fe-depleted HFHS 4936.85
143 cal/g; Fe-enriched HFHS 4886.9 cal/g). Dietary protein content was determined by combustion (Dumas
144 method) using a LECO FP-528 apparatus (LECO Corporation, St. Joseph, MI, USA) and was 14.75% [w/w]
145 for Fe-depleted LFLS, 14.31% for Fe-enriched LFLS, 18.79% for Fe-depleted HFHS, and 18.16% for Fe-
146 enriched HFHS. Dietary fat content was measured with an ANKOMXT10 Extractor (ANKOM
147 Technology, Macedon, NY, USA) and was different between the diets, reflecting the fact that we have low-
148 fat and high-fat diet (Fe-depleted 12 mg/kg LFLS 3.81% [w/w]; Fe-enriched 150 mg/kg LFLS 4.25%
149 [w/w]; Fe-depleted 12 mg/kg HFHS 21.62% [w/w]; Fe-enriched 150 mg/kg HFHS 22.13% [w/w]). Animals
150 were fed *ad libitum* with these diets for 28 days and had access to *ad libitum* water. Body weight and food
151 intake were monitored twice weekly. Mice were killed by cardiac puncture. Whole blood was collected in
152 K3-EDTA tubes to obtain plasma (1,780 × g, 10 min). Ileum and caecum tissues were collected at 10 cm
153 and 2 cm from the ileocecal junction, respectively. Luminal contents were collected in PBS by gentle
154 scraping. Tissue samples from both ileum and caecum were treated with RNAlater Stabilization Solution
155 (ThermoFisher, USA) to preserve the integrity of RNA until its subsequent extraction. All samples were
156 stored at -80°C until further analysis.

157

158 **Endocannabinoidome quantification**

159 Lipids were extracted from plasma samples (40 µL) as in (Turcotte et al., 2020). In brief, plasma samples
160 were diluted to a volume 500 µL with Tris buffer (50 mM, pH=7). 5 µL of deuterated standards were added
161 to each sample then vortexed. Two millilitres of toluene were then added, and samples were vortexed for
162 30 seconds. Samples were next placed in a dry ice-ethanol bath to freeze the aqueous phase. The toluene
163 phase was then collected and evaporated to dryness under a stream of nitrogen. Ileum and caecum samples
164 (5 to 10 mg) were extracted and processed exactly as in (Manca et al., 2020). All lipid extracts were then
165 resuspended with 60 µL of mobile phases (50% Solvent A and 50% solvent B) then injected (40 µL) on the
166 injected onto an HPLC column (Kinetex C8, 150 × 2.1 mm, 2.6 µM; Phenomenex) as described before
167 (Everard et al., 2019). Quantification of eCBome-related mediators was performed using a Shimadzu 8050
168 triple quadrupole mass spectrometer. The following metabolites were quantified: 1/2-oleoyl-glycerol (2-
169 OG), 1/2-linoleoyl-glycerol (LG), 1/2-arachidonoylglycerol (2-AG), 1/2-eicosapentaenoyl-glycerol (2-
170 EPG), 1/2-docosapentaenoyl(n-3)-glycerol (2-DPG), 2-docosahexaenoylglycerol (1/2-DHG), *N*-palmitoyl-
171 ethanolamine (PEA), *N*-stearoyl ethanolamine (SEA), *N*-oleoyl ethanolamine (OEA), *N*-linoleoyl-
172 ethanolamine (LEA), *N*-arachidonoyl ethanolamine (AEA), *N*-eicosapentaenoyl ethanolamine (EPEA), *N*-
173 docosapentaenoyl ethanolamine (DPEA), *N*-docosahexaenoyl ethanolamine (DHEA), arachidonic acid

174 (AA), docosaehaenoic acid (DHA), docosaepentaenoic acid (DPA), eicosapentaenoic acid (EPA),
175 stearidonic acid (SDA), linoleic acid (LA), PGD₂, PGE₁, PGE₂, PGE₃, 1a,1b-dihomo PGF_{2α} (1a,1b-dihomo
176 PGF_{2α}), thromboxane B₂ (TBX), *N*-Palmitoyl-Glycine and *N*-Oleoyl-Serotonin. For the MAGs, the signals
177 from the *sn*-1(3) and the *sn*-2 isomers were combined and presented as 2-MAGs, in order to take into
178 account the rapid isomerization of the *sn*-2 isomer to *sn*-1(3).

179

180 **16S rRNA gene sequencing**

181 Intestinal luminal contents were lysed using bead beating (0.1 mm silica beads) before enzymatic digestion
182 with 50 mg of lysozyme and 200 U/μL mutanolysin (37°C, 45 min). Microbial DNA was extracted using
183 the QIAamp DNA Stool minikit (Qiagen, CA, USA), and amplification of the V3-V4 region was performed
184 using the primers Bact-0341-b-S-17 (5'-CCTACGGGNGGCWGCAG-3') and Bact-0785-a-A-21 (5'-
185 GACTACHVGGGTATCTAATCC-3') (Illumina, CA, USA). Libraries were purified using magnetic beads
186 AMPURE XP (Beckman Coulter Canada Lp), and libraries were assessed on gel using QIAexcel (Qiagen,
187 CA, USA). High-throughput sequencing (2- by 300-bp paired end) was performed on a MiSeq platform
188 (Illumina, CA, USA). Sequences were processed using the DADA2 package (version 1.16.0) (Callahan et
189 al., 2016) and associations with bacterial taxa were obtained using the Ribosomal Database Project
190 reference database Silva version 132. Microbiome abundances were normalized using rarefaction
191 (Rarefaction; Vegan R package). Reads were rarefied to 5000 reads to account for depth bias (McMurdie
192 & Holmes, 2014). Samples with read count lower than 5000 but higher than 2000 reads were kept in the
193 analysis as is. Prior to rarefaction, we observed 5113 ASV and after rarefaction we observed 4923 ASV.
194 Raw sequences were deposited to SRA under accession PRJNA977215
195 (<https://www.ncbi.nlm.nih.gov/bioproject/PRJNA977215/>).

196

197 **mRNA isolation, reverse transcription and qPCR**

198 RNA was extracted from the ileum and caecum samples with the RNeasy Plus mini kit (Qiagen, CA, USA)
199 according to the manufacturer's instructions and eluted in 30 μL of UltraPure distilled water (Invitrogen,
200 USA). RNA concentration and purity were determined by measuring the absorbance of RNA in a nanodrop
201 at 260 nm and 280 nm. A total of 500 nanograms of RNA was reverse transcribed with a high-capacity
202 cDNA reverse transcription kit (Applied Biosystems, CA, USA). We used 7500 Real-Time PCR System
203 (Applied biosystems, CA, USA) to perform quantitative PCR to assess the expression of 2 genes associated
204 with anti-inflammatory activity (*Il10* and *Tgfb1*) and 2 genes associated with pro-inflammatory activity
205 (*Il1b* and *Tnfa*) with one housekeeping gene (*Hprt*). Primers and probes for TaqMan qPCR assays were
206 purchased as commercial kits (ThermoFisher Scientific, Burlington, ON, Canada) and TaqMan assay IDs
207 were as follows: *Hprt* (Mm03024075_m1), *Il10* (Mm01288386_m1), *Tgfb1* (Mm01178820_m1), *Il1b*

208 (Mm00434228_m1), and *Tnfa* (Mm00443258_m1). All expression data were normalized by the threshold
209 cycle ($2^{-\Delta\Delta CT}$) method using *Hprt* as internal control (Livak & Schmittgen, 2001).

210

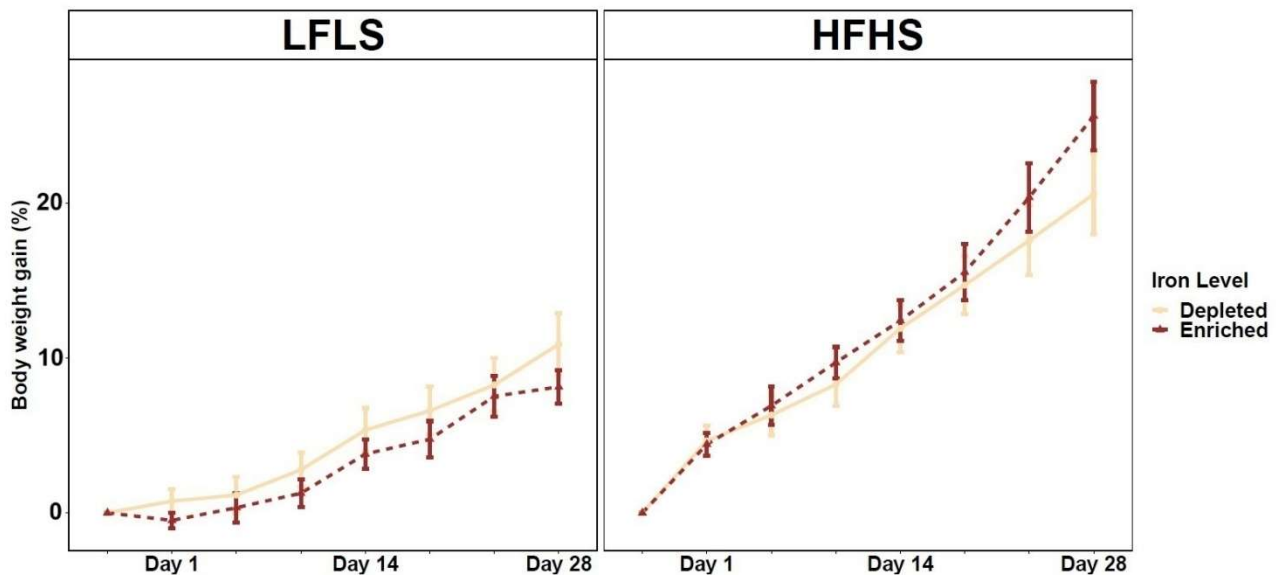
211 **Statistical analyses**

212 Data are expressed as mean \pm SEM. Generalized linear regression models were used to identify the effects
213 of Fe, diet and sex on ranked values of eCBome mediators and gut microbiome relative abundances. We
214 used a three-way ANOVA based on a linear model that included interactions between diet formulation
215 (LFLS vs HFHS), Fe concentration (depleted vs enriched) and sex of the animal (female or male). The
216 differences were considered statistically significant with P values of $P < 0.05$ using contrast tests between
217 Fe-depleted and Fe-enriched levels, LFLS and HFHS formulations, the sex of animals (female and male)
218 and the combination between Fe levels and diet formulations. Spearman correlations were used to
219 investigate associations between microbiome families and eCBome mediators. Adjustments for multiple
220 testing were obtained using false-discovery rate (FDR). Analyses were performed with R software version
221 4.0.2. Principal-component analysis was performed using the FactoMineR R package (Lê et al., 2008).
222 PERMANOVA was performed between two of the segments of the intestine (ileum and caecum) with 999
223 permutations in conjunction with Canberra distances between samples using package vegan in R (v2.5.7).

224

225 **Results:**226 **Dietary Fe intake has no impact on weight gain.**

227 Variations in dietary Fe intake showed no clear effect on the weight gain of the mice after 28 days. However,
 228 as expected, mice fed with HFHS diets showed an increase in weight in comparison with LFLS, regardless
 229 of Fe intake (Figure 1). As for sex differences, male mice showed a greater weight gain than females on
 230 both type of Fe-enriched and Fe-depleted diets (Figure S1). These results suggest that Fe has a limited
 231 impact on weight gain in mice for the period of treatment.



232

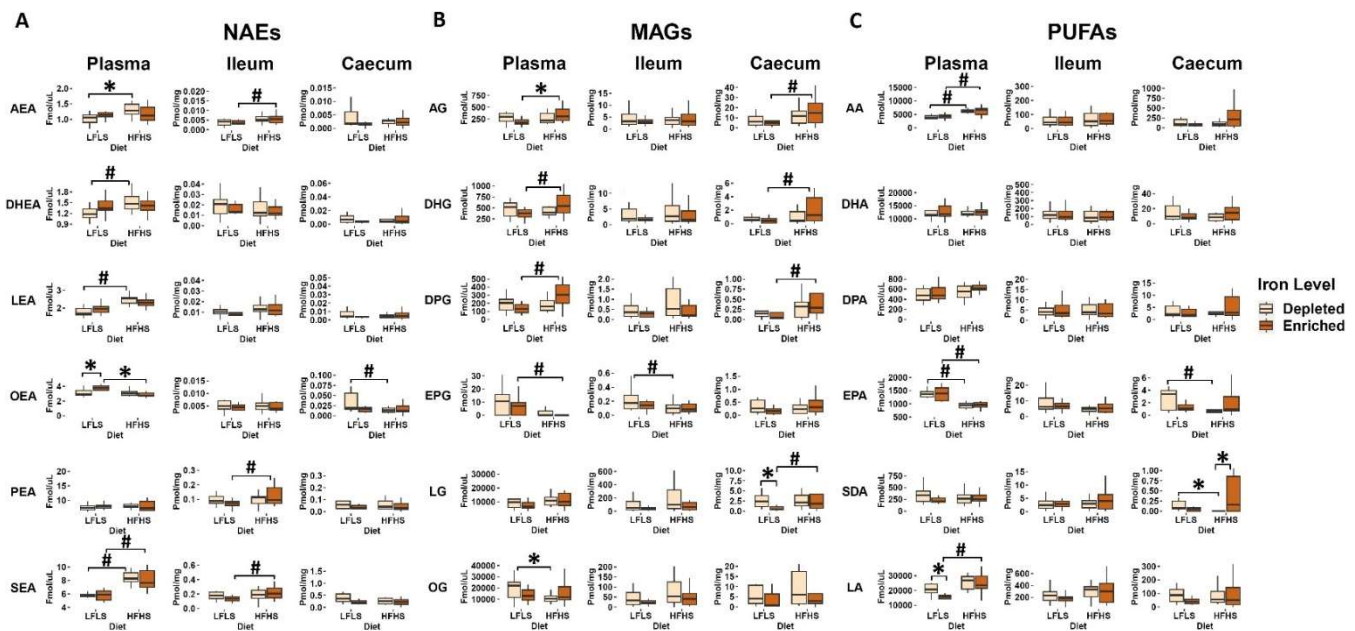
233 **Figure 1. Weight gain in mice fed Fe-enriched and Fe-depleted LFLS or HFHS diets.** Groups of 12
 234 mice (6F/6M) were fed Fe-enriched /or Fe-depleted diets combined with LFLS or HFHS diet for 28 days.
 235 Generalized linear regression models were used to identify the effects of Fe and macronutrient diet
 236 formulation interactions on weight gain (%) over time for 28 days of study. Data are expressed as mean \pm
 237 SEM (n = 12).

238

239 **Dietary iron influences circulating *N*-acylethanolamine production in interaction with diet**
 240 **composition.**

241 We quantified the eCBome mediators (NAEs, MAGs) and some of their corresponding polyunsaturated
 242 fatty acids (PUFAs) in plasma, ileum, and caecum samples (Figure 2). As observed in previous work, the
 243 eCBome response was different between plasma and the two intestinal segments studied (Guevara Agudelo
 244 et al., 2022). Macronutrient composition of the diet was the main driver of eCBome concentrations, and
 245 modulation by diet and Fe intake was not homogeneous between tissues. Overall, the influence of Fe on
 246 NAEs, MAGs and PUFAs was always observed in interaction with the diet. Indeed, OEA showed a
 247 significant increase associated with the enrichment of Fe in LFLS diet whereas lower OEA concentrations

248 were observed in the other conditions (Figure 2A). Circulating levels of MAGs were also modulated by Fe
 249 in interaction with diet composition. For instance, we observed that 2-AG was reduced in Fe-enriched LFLS
 250 diet compared to Fe-enriched HFHS diet. By contrast, 2-OG was increased in Fe-depleted LFLS diet
 251 compared to HFHS diet. Interestingly, significant increase of the PUFA LA was associated with the
 252 depletion of Fe in the diet in combination with LFLS (Figure 2C). Caecum SDA showed a statistically
 253 significant reduction associated with Fe depletion in HFHS diet. These results suggest a differential role of
 254 Fe intake and its interaction with dietary fat and sucrose levels in modulating the concentration of some
 255 eCBome mediators or their corresponding fatty acids. Several fatty acids and eCBome mediators were
 256 modulated solely by the diet. Circulating 2-DHG, 2-DPG, DHEA, LEA, and SEA showed an increase
 257 associated strictly with HFHS diets, while 2-EPG, as well as its precursor EPA, showed a reduction
 258 associated with HFHS diets. In the intestine, we observed that modulation of most NAEs and MAGs and
 259 their corresponding PUFAs were associated with dietary fat content and not dietary Fe levels. In the ileum,
 260 AEA and SEA were higher with HFHS than the LFLS diet. By contrast, in the caecum, EPA showed an
 261 increase with LFLS. 2-AG, 2-DHG, 2-DPG and 2-LG levels were higher with the HFHS than the LFLS
 262 diet. Overall, these results indicate that Fe, in interaction with the macronutrient composition of the diet,
 263 influences the production of circulating NAEs, while the formulation of HFHS diets mainly increased
 264 MAGs in the intestine.

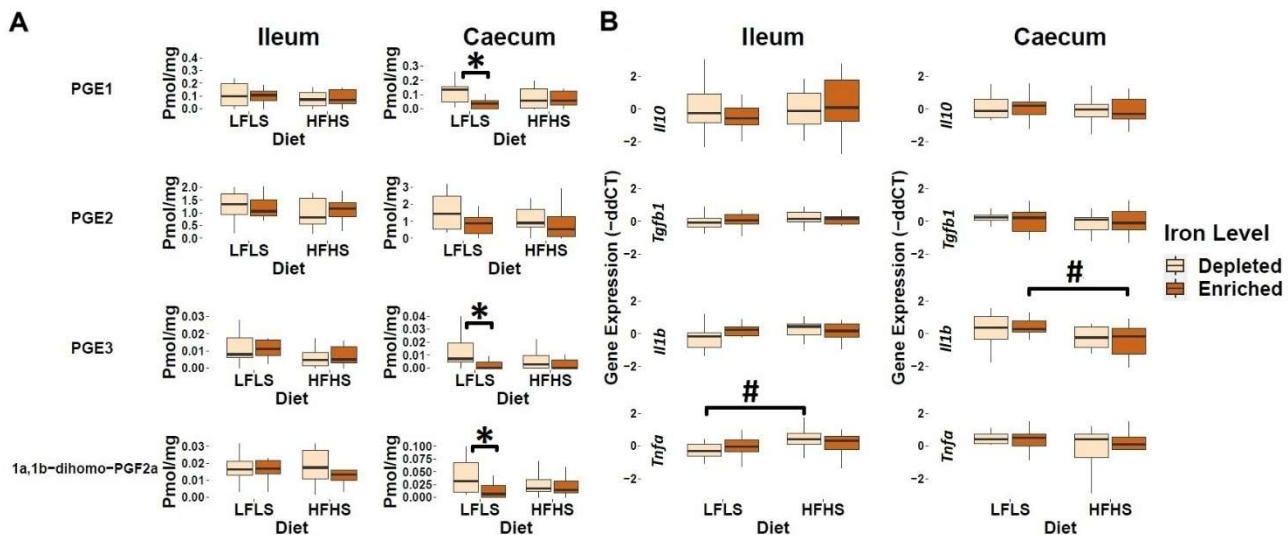


265
 266 **Figure 2. Diet and Fe modulation of endocannabinoidome mediators and some of their corresponding**
 267 **fatty acids.** Boxplot representation of the eCBome mediators A) *N*-acylethanolamines (NAEs), B) 2-
 268 monoacylglycerols (2-MAGs), and C) long chain ω -6 and ω -3 polyunsaturated fatty acids (PUFAs)
 269 response to Fe-depleted and Fe-enriched LFLS or HFHS diets. Data are expressed as the mean \pm SEM
 270 ($n = 12$). *P* values of linear contrast analysis are detailed when significant ($p < 0.05$) using contrast tests

271 between enriched and depleted Fe levels, LFLS and HFHS formulations and the combination between Fe
 272 levels and formulations. The star '*' symbol was used to show the effect of Fe alone or in interaction with
 273 LFLS or HFHS. The numeral '#' symbol was used to denote the effect of only LFLS or HFHS. The samples
 274 were analyzed at day 28 of the study.
 275

276 Iron modulates the concentration of caecal prostaglandins with the LFLS diet.

277 In addition to endocannabinoid congeners and PUFAs, we also quantified lipid mediators that could respond
 278 differentially to dietary intake of Fe. In this sense, we evaluated the response of PGE₁, PGE₂, PGE₃ and
 279 1a,1b-dihomo PGF_{2α} (Figure 3). In the caecum, we observed that the enrichment of Fe in the diet decreased
 280 the levels of prostaglandins PGE₁, PGE₃ and 1a,1b-dihomo PGF_{2α}. PGE₂ exhibited a similar trend of
 281 reduction with Fe enrichment but did not display a significant difference. We did not observe this effect in
 282 the ileum (Figure 3A). In the intestine, expression of genes involved in inflammation was not influenced
 283 by dietary Fe intake, but rather by diet formulation (Figure 3B). For instance, in the ileum, we observed an
 284 increase of *Tnfa* expression levels only in those mice fed with the HFHS diet with depleted Fe, while in the
 285 caecum this increase was not evident. In addition, the expression of *Il1b* was significantly increased by the
 286 LFLS diet in caecum. Taken together, these results point to a possible role of Fe intake in intestinal immune
 287 response by modulating the production of bioactive lipids such as prostaglandins, although with limited
 288 effect on the intestinal expression of inflammation-associated genes.



289

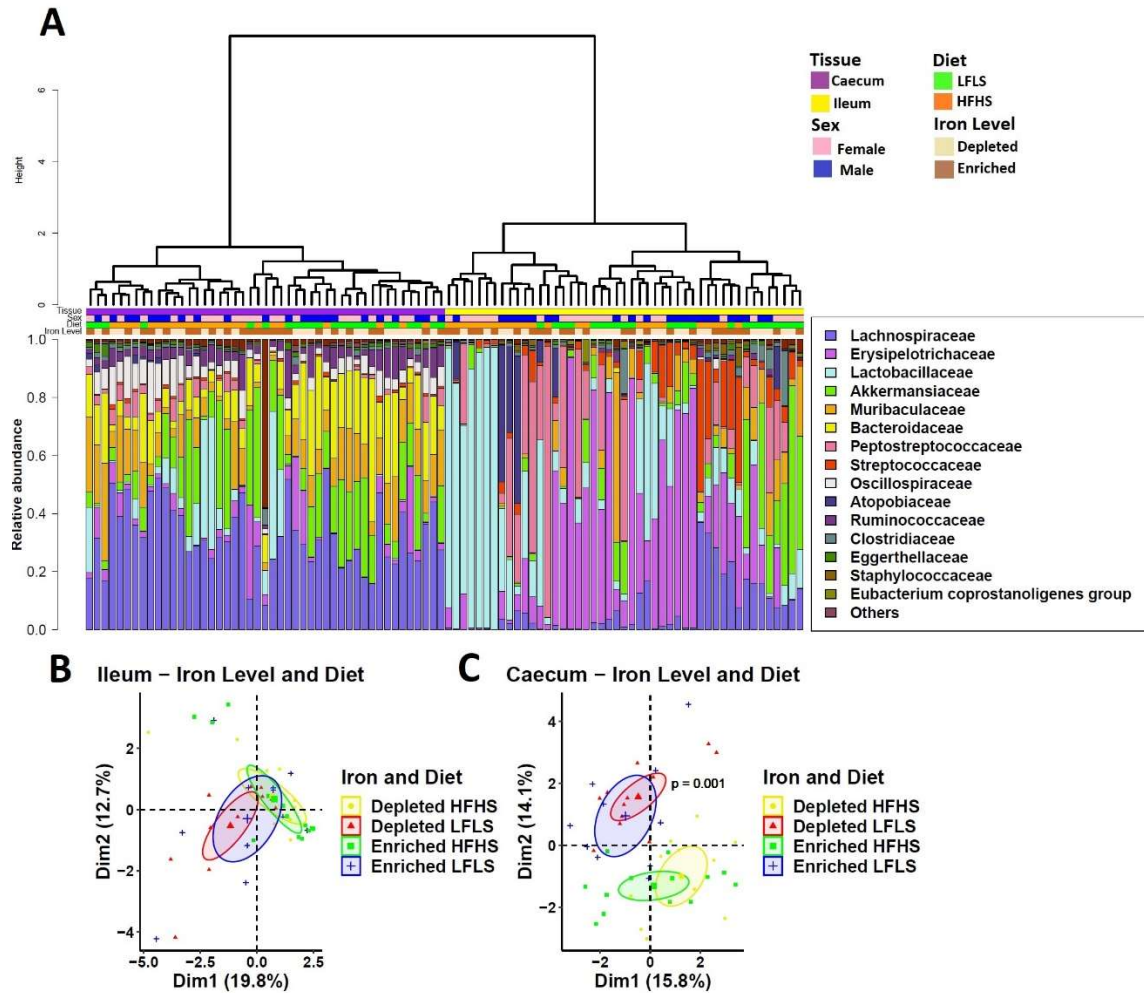
290 **Figure 3. Response of intestinal prostaglandins and mRNA gene expression of immune response in**
 291 **Fe-depleted and Fe-enriched LFLS or HFHS diets in the intestine.** Boxplot representation of the
 292 eCBome mediators in (A) ileum and (B) caecum. mRNA expression of immune response as fold change
 293 (FC) calculated using the $\Delta\Delta C_T$ method in Fe-depleted and Fe-enriched LFLS or HFHS diets in the
 294 intestine, ileum, and caecum. Data are expressed as the mean \pm SEM (n = 12). P values of linear contrast
 295 analysis are detailed when significant (p<0.05) using contrast tests between enriched and depleted Fe levels,
 296 LFLS and HFHS formulations and the combination between Fe levels and formulations. Gene expression
 297 was normalized to *Hprt*. The star '*' symbol was used to show the effect of Fe alone or in interaction with

298 LFLS or HFHS. The numeral '#' symbol was used to denote the effect of only LFLS or HFHS. The samples
299 were analyzed at day 28 of the study.

300

301 **Iron affects specific microbial species in interaction with the diet**

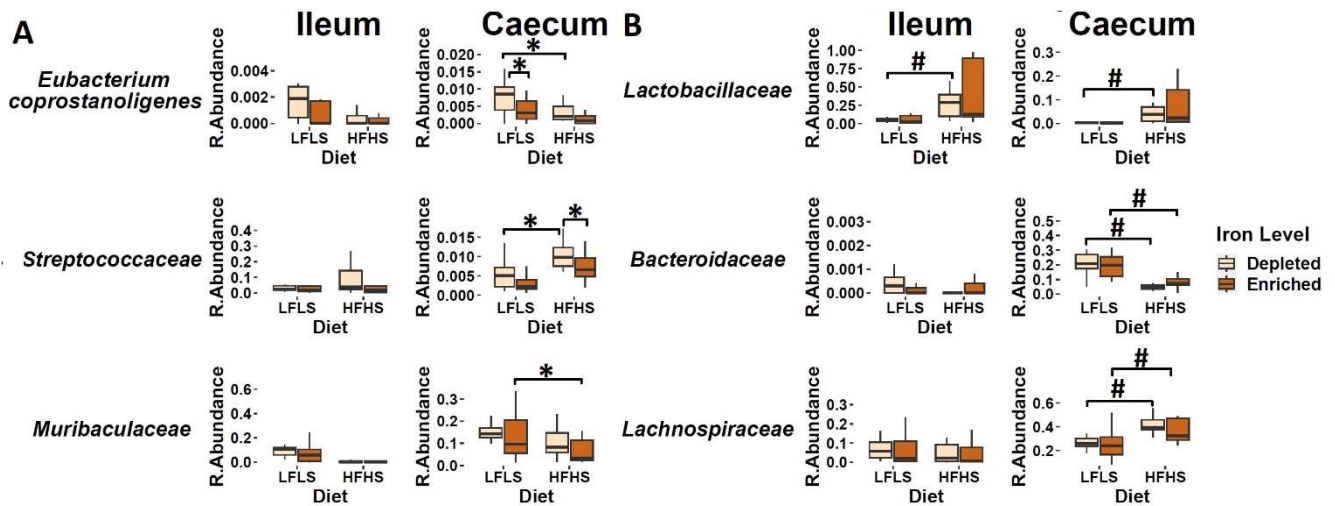
302 We investigated whether specific gut microbial families responded differentially to dietary Fe enrichment
303 and whether these associations were dependent on fat and sucrose intake. As observed previously (Guevara
304 Agudelo et al., 2022), the intestinal microbiota composition showed a remarkable differentiation between
305 the segments of the intestine ($p < 0.01$, PERMANOVA) (Figure 4A). Interindividual differences of microbial
306 taxa were more pronounced in the ileum than in the caecum, which was more homogeneous. Thus, in the
307 ileum, microbiome did not show a clear influence of Fe or diet (Figure 4B), while in the caecum the
308 difference was evident between LFLS and HFHS diets (Figure 4C). Three intestinal microbial families
309 (*Eubacterium coprostanoligenes* group, *Streptococcaceae* and *Muribaculaceae*) responded directly to Fe
310 intake or interaction between Fe and diet content exclusively in caecum, as in the ileum no microbial family
311 responded to the dietary changes in Fe, be it alone or in interaction with diet. For instance, *Eubacterium*
312 *coprostanoligenes* group bacteria showed an increase in its relative abundance associated with the
313 interaction of Fe-depletion with LFLS diets. Similarly, the relative abundance of *Streptococcaceae* was
314 higher with the interaction between the depletion of dietary Fe with the HFHS formulation (Figure 5A).
315 Concomitantly, *Muribaculaceae* showed a slight increase in its relative abundance due to the interaction of
316 Fe-enrichment with LFLS formulations. Other microbial families in the ileum such as *Lactobacillaceae*
317 responded to the macronutrient content of the diet and exhibited a higher abundance with HFHS diets.
318 *Bacteroidaceae* was more abundant with the LFLS diet, and *Lachnospiraceae* was increased with HFHS
319 diet (Figure 5B). Interestingly, increased abundance of both microbial taxa occurred only in Fe-depleted
320 diets. Taken together, these results indicate that Fe, in interaction with diet formulation, shifted specific
321 microbial families in an intestinal segment-dependent manner.



322
 323

324 **Figure 4. Intestinal microbiota composition in response to Fe-enriched and Fe-depleted LFLS or**
 325 **HFHS diets.** A) Relative bacterial abundance at the family level in response to Fe-enriched and Fe-depleted
 326 LFLS or HFHS diets in ileum and caecum. Families representing less than 1% of total bacterial abundance
 327 were aggregated. Dendrogram showing hierarchical clustering based on Canberra distance between samples
 328 determines the sample order. The corresponding annotations for tissue, sex, diet, and Fe level are displayed.
 329 Principal component analysis shows the impact of Fe-depleted/enriched and LFLS/HFHS diets on gut
 330 microbiota composition in the B) ileum, and C) caecum. PERMANOVA indicates significance of
 331 microbiota composition between the dietary conditions. The samples were analysed at day 28 of the study.

332



333

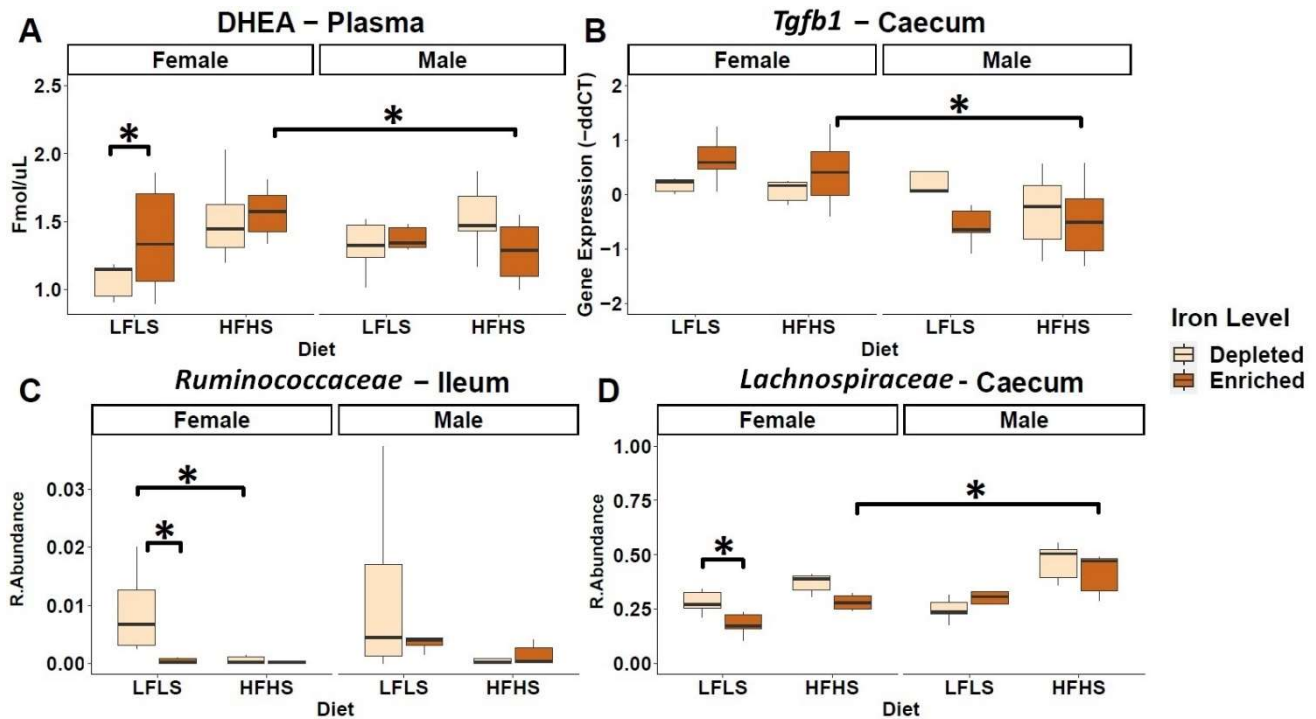
334 **Figure 5. Effect of Fe-depleted and Fe-enriched LFLS or HFHS diets on bacterial relative abundance**
 335 **at the family level in the ileum and caecum.** A) Effect of Fe in interaction of LFLS and HFHS
 336 formulations on intestinal microbial families. B) Effect of solely LFLS or HFHS formulations. Data are
 337 expressed as the mean \pm SEM (n = 48). P values of linear contrast analysis are detailed in the bottom when
 338 significant ($p < 0.05$) using contrast tests between enriched and depleted Fe levels, LFLS and HFHS
 339 formulations and the combination between Fe levels and formulations. The star '*' symbol was used to
 340 show the effect of Fe alone or interaction with LFLS or HFHS. The numeral '#' symbol was used to denote
 341 the effect of only LFLS or HFHS. The samples analyzed and showed are at day 28 of the study.

342

343 **Dietary Fe in interaction with sex influences circulating N-acyl ethanolamines, cytokine gene** 344 **expression and specific intestinal bacteria**

345 In addition to the impact of dietary Fe and diet formulations, we studied the effect of Fe and its interaction
 346 with the sex of the animals regarding the changes in the production of eCBome mediators, intestinal
 347 cytokine gene expression and gut microbiota species. We found that circulatory levels of DHEA showed
 348 an interaction between Fe-depletion and the sex of the animal, such as reduced DHEA levels in Fe-depletion
 349 was observed only in females (Figure 6A). Concomitantly, we found a significant increase in the expression
 350 levels of *Tgfb1* in females compared to males under the interaction between the Fe-enriched diets with the
 351 HFHS formulation (Figure 6B). Similarly, microbial families such as *Ruminococcaceae* and
 352 *Lachnospiraceae* exhibited a reduction in their relative abundance associated to the interaction between Fe
 353 enrichment in diets and female mice. In addition, the reduction of Fe in the diets increased the relative
 354 abundance of specific microbial families in female mice such as *Lachnospiraceae* and *Ruminococcaceae*.

355 Furthermore, *Lachnospiraceae* family showed an increase in males over females with Fe-enriched diets
 356 and the HFHS diet.



357 **Figure 6. Iron influences in a sex-dependent manner circulating *N*-acylethanolamines (NAEs),**
 358 **cytokine gene expression and intestinal microbial species.** A) Boxplot representation of the NAEs in
 359 plasma, B) mRNA expression of *Tgfb1* as fold change (FC) calculated using the $\Delta\Delta C_T$ method, C) relative
 360 abundances of *Ruminococcaceae* in the ileum and D) *Lachnospiraceae* in the caecum. Data are expressed
 361 as the mean \pm SEM (n = 48). *P* values of linear contrast analysis are marked with a star “*” when significant
 362 ($p < 0.05$) using contrast test between enriched and depleted Fe levels, LFLS and HFHS formulations, the
 363 combination between Fe levels and formulations, and the sex of the animal.
 364

365 Discussion

366 In this study, we investigated the effect of Fe depletion (12 mg/kg) and enrichment (150 mg/kg),
 367 in interaction with macronutrients (LFLS or HFHS), on the eCBome and gut microbiota in a mouse model
 368 susceptible to obesity. In contrast with several studies that used bleedings or diets with less than 6 mg Fe/kg
 369 to characterize the metabolic defects associated with severe Fe deficiency (B R Blakley, 1988; Cooksey et
 370 al., 2010; Santos et al., 1998), we did not target severe dietary Fe depletion, and the model used here did
 371 not provoke either anemia in the Fe-depleted diets or hemochromatosis in the Fe-enriched diets. The present
 372 study could be considered short-term as it was only 4 weeks-long. Although our aim was not to produce
 373 systemic and tissue inflammation, previous studies have shown that 4 weeks of an obesogenic diet in mice
 374 is enough to alter the inflammatory phenotype and provoke changes in gut microbiota. (Cani et al., 2009;
 375 Guevara Agudelo et al., 2022).

376 The results obtained here suggest that short-term Fe administration may have little direct effect on
377 body weight modulation, since there was no weight gain associated with either the enrichment or depletion
378 of Fe during the length of the study. The fact that caloric intake did not increase significantly after Fe
379 supplementation could explain the lack of Fe-associated weight gain. It is possible that the interaction
380 between Fe and other nutrients may have affected weight gain in comparison with other studies using
381 different diets (Lynch & Cook, 1980; Piskin et al., 2022). In this regard, Fe absorption may be influenced by
382 the presence of other nutrients in the diet, which were not investigated. Yet, there is increasing evidence
383 that obesity and Fe status are connected (Cepeda-Lopez et al., 2013; Kitamura et al., 2021), as human
384 studies report a reduction in Fe plasma levels with increasing adiposity (Manios et al., 2013; Seltzer &
385 Mayer, 1963; Wenzel et al., 1962). Indeed, long-term treatment of Fe deficiency anemia for 4-6 months by
386 increasing Fe gradually induced weight loss (Aktas et al., 2014). Besides, it has also been reported that Fe
387 supplementation for 15 weeks reduces diet-induced weight gain (Kitamura et al., 2021), with significant
388 changes being observed from 12 weeks of treatment.

389 Accumulating evidence has revealed a strong link between dietary Fe and lipid metabolism
390 (Cunnane & McAdoo, 1987; Zhou et al., 2011). In fact, fatty acid composition in tissues can be modified as
391 a consequence of nutritional Fe deficiency (Johnson et al., 1989). Furthermore, the role of Fe in fatty acid
392 desaturation has been demonstrated (Romero et al., 2018). Previous studies have also shown the production
393 of ω -6 PUFAs, particularly LA, can be regulated by dietary Fe levels (Ananda Rao et al., 1980).
394 Concordantly, we found a significant increase in LA associated with dietary Fe-enrichment in combination
395 with LFLS (Figure 2C). We evaluated the effect of Fe intake in interactions with low or high calory diets
396 on the circulating and intestinal levels of the most studied eCBome mediators (NAEs and MAGs), and some
397 of their corresponding PUFAs. The eCBome is known to be highly influenced by dietary intake as well as
398 by body composition (Castonguay-paradis et al., 2020). It is understood to play an important role in
399 physiological processes related to metabolic health (Di Marzo, 2018). In this study, the influence of Fe on
400 NAEs, MAGs and PUFAs was always observed in interaction with diet formulations. Indeed, OEA showed
401 a significant increase associated with the enrichment of Fe in LFLS diet only, with the other conditions
402 having lower, and comparable OEA concentrations (Figure 2A). As expected, circulating levels of AEA
403 were higher with the HFHS diet (Lacroix et al., 2019), but interestingly this difference was more
404 pronounced in interaction with Fe-depletion, as it was for DHEA. Recently, there has been growing interest
405 in a group of NAEs that are congeners of AEA but that seem instead to act through mechanisms independent
406 of cannabinoid receptors. This group includes the monounsaturated analog OEA (Piomelli, 2013; Romano
407 et al., 2014), which share biosynthetic and catabolic pathways with AEA (Okamoto et al., 2004) but exerts
408 contrary effects on the regulation of food intake and lipid metabolism. Unlike AEA, OEA has no binding
409 affinity to the CB₁ receptor (V M Showalter, 1996) and its administration reduces food consumption in

410 rodents. Supplementation with Fe has been associated with increased appetite and food intake
411 independently of weight gain (Gao et al., 2015). In this study, we found a significant increase in OEA levels
412 associated with Fe enrichment in the LFLS diet, although there was no significant correlation between
413 circulating OEA levels and food intake ($p = 0.81$, Spearman correlation). Recent studies have shown that
414 OEA acts as a gut-derived satiety factor (De Filippo et al., 2023; Gaetani et al., 2010) and might be involved
415 in eating disorders (Gaetani S, 2008), obesity (Matias et al., 2012) and type 2 diabetes (Annuzzi et al.,
416 2010). Among other functions, OEA controls the secretion of GLP-1, suggesting a synergistic action of this
417 NAE with intestinal microorganisms in the regulation of several homeostatic functions, since GLP-1 has
418 numerous metabolic actions including decreased gastric clearance, inhibition of food intake, and
419 stimulation of glucose-dependent insulin secretion (Müller et al., 2019). Results of this study suggest that
420 Fe intake may modulate circulating OEA levels and this point out to the possibility of dietary interventions
421 to increase levels of this mediator and, hence, affect its main receptors, i.e. the peroxisome proliferator-
422 activate receptor α (PPAR α), the transient receptor potential vanilloid of type 1 (TRPV1) channel, and the
423 G-protein-coupled receptor 119 (GPR119), all of which are known to counteract obesity (Christie et al.,
424 2018; Grimaldi, 2001).

425 Several 2-MAGs, including 2-AG, 2-DPG and 2-DHG, showed higher concentrations with Fe-
426 enriched HFHS diet compared to Fe-enriched LFLS diet both in plasma and in the caecum, but not in the
427 ileum. These mediators have been linked to the modulation of metabolic activity and inflammation (Barrie
428 & Manolios, 2017; Hillard, 2017; Poursharifi et al., 2017). Intestinal 2-MAG metabolism is tightly linked
429 to re-esterification to triacylglycerol and crosstalk between Fe and lipid pathways, including alterations in
430 cholesterol, sphingolipid, and lipid droplet metabolism in response to in Fe levels have been reported (Chon
431 et al., 2007; Rockfield et al., 2018). In a previous study, we investigated the impact of the trace mineral
432 selenium (Se) on the eCBome (Guevara Agudelo et al., 2022). Although Se had a significant effect on
433 weight gain particularly under a LFLS diet, it showed an opposite effect to Fe in its impact on intestinal 2-
434 MAGs levels. Notably the levels of mediators such as 2-AG, 2-DHG and 2-DPG in the caecum were
435 favoured in Se-depleted HFHS diets, whereas, in the present study, we observed that these mediators were
436 increased by the HFHS diet only in the presence of Fe supplementation (Figure 2B). Given the association
437 between tissular 2-AG levels and dysmetabolism, observed also in humans (Silvestri & Di Marzo, 2013), it
438 is tempting to speculate that individuals may be protected by the negative effects of a cafeteria-type diet
439 with supplementation of Se and slight reduction of dietary Fe.

440 Fe is an important cofactor involved in the synthesis of AA, which plays functions associated with
441 cell signalling and serves as a precursor of numerous oxygenated derivatives such as the prostaglandins.
442 The fact that we have identified increased circulating PUFAs and 2-MAGs is consistent with Fe proposed
443 involvement in immune response (Nairz & Weiss, 2020). Indeed, during Fe-supplementation, increased

444 release of AA and eicosanoids have been associated with lipid oxidation reactions (Peterson et al., 1978),
445 and prostaglandin metabolism (Mattera et al., 2001; Wright & Fischer, 1997). We observed reduced levels
446 of PGE₁ and PGE₃ as well as a trend for reduced levels of PGE₂ in the caecum with the Fe-enriched LFLS
447 diet, suggesting lowered inflammation in this tissue. These effects were not observed in the ileum, which
448 possibly reflects the lack of changes observed in this tissue of the biosynthetic precursors of PGE₂ (AA and
449 possibly 2-AG) and of PGE₃ (EPA and possibly 2-EPG) and the increase of the pro-inflammatory cytokine,
450 *Tnfa*, with the Fe-depleted HFHS.

451 Bioavailability of Fe in the gut lumen also plays an important role for the microbes that reside in this
452 dynamic environment (Seyoum et al., 2021). Competition for its acquisition takes place at the intestinal
453 host-bacteria interface (Nairz et al., 2010; Yilmaz & Li, 2018). Fe availability is known to be critical for
454 bacterial growth, and Fe starvation is an effective strategy to limit bacterial survival. Nutrients from the diet
455 are absorbed in different sections of the intestine (Kiela & Ghishan, 2016), which promotes specific
456 microbial niches (Pereira & Berry, 2017). In microorganisms, Fe serves as a cofactor for proteins involved
457 in key microbial metabolic pathways such as redox reactions, DNA synthesis and the production of short-
458 chain fatty acids (SCFA) (Dostal et al., 2015) and, subsequently, the proliferation and growth of almost all
459 microbiota, including both the commensal and pathogenic species, are dependent on the utilization of
460 unabsorbed dietary Fe. We report here that a limited number of microbial families exhibited different
461 relative abundances based on Fe and macronutrient intake. While intestinal microbiota composition
462 displayed a remarkable differentiation between the segments of the intestine, differences in microbiome
463 composition associated with Fe intake were observed in the caecum but not in the ileum. Here we found
464 that the *Eubacterium coprostanoligenes* group, a cholesterol-reducing intestinal bacterium that synthesizes
465 coprostanol (Juste & Gérard, 2021), and *Streptococcaceae* both show an increase in their relative abundance
466 following Fe-depletion but under different macronutrient combinations. This suggests the presence of
467 macronutrients may be necessary for the adaptation of some microbial species to the changes in the
468 bioavailability of intestinal micronutrients (Sung et al., 2023). By contrast, we found that *Muribaculaceae*
469 shows an increase in its relative abundance during Fe-enrichment in combination with LFLS diets, which
470 had already been observed in a previous study (Ippolito et al., 2022). Other microbial families, including
471 *Lactobacillaceae*, *Bacteroidaceae* and *Lachnospiraceae*, responded exclusively to dietary formulations and
472 not to Fe intake (Figure 5B). Interestingly, *Lactobacillus* were found by Dostal and collaborators to be
473 modulated by Fe in mice given a chow diet (Dostal et al., 2012), strengthening the idea that the interaction
474 between micronutrients and macronutrients is a key element in microbiome modulation. Taken together,
475 these results highlight the fundamental shaping factor exerted by diet on intestinal populations. Finally,
476 although dietary components other than Fe levels were determinant for the differential production of

477 eCBome mediators and intestinal microbial families, the sex of the mice also impacted both systems, which
478 is consistent with previous findings (Guevara Agudelo et al., 2022).

479

480 **Conclusions**

481 Overall, our results indicate that the macronutrient composition of the diet modulates the response of the
482 eCBome and the microbiome to Fe intake in mice, a phenomenon that was also observed for selenium,
483 another trace mineral (Guevara Agudelo et al., 2022). Specifically, an increase in circulating levels of OEA
484 was associated with Fe enrichment in the LFLS diet, concomitantly with a decreased concentrations of
485 plasma LA, caecal prostaglandins and the caecal abundance of *Eubacterium coprostanoligenes*, potentially
486 in reaction to Fe availability in a less dietary rich environment. By contrast, the Fe-depleted HFHS diet
487 showed an elevation of AEA, which is usually associated with negative metabolic health outcomes. This
488 suggests a crosstalk between the amounts of trace minerals and the dietary macronutrient content to generate
489 a differential impact on the levels of eCBome mediators and their potential role in metabolic complications.
490 In conclusion, our findings show that Fe might, in interaction with the diet, modulate intestinal processes
491 as well as the host response to dietary stress. This study demonstrates how complex is the interplay between
492 dietary components, the gut microbiota ecosystem and host lipid signaling systems. The present findings
493 should open the path for mechanistic studies exploring the molecular basis of the impact of macronutrients
494 on the gut microbiome-eCBome axis, in response to Fe deficit or supplementation, and the role of this
495 interaction in low-grade inflammation such as that accompanying diet-induced obesity.

496

497 **Financial Support**

498 This work was carried out within the activities of the Canada Excellence Research Chair in Microbiome-
499 Endocannabinoidome Axis in Metabolic Health, held by V. Di Marzo and funded by the Canadian Federal
500 Government Tri-Agency (CERC programme) and the CFI Leaders fund. FR is funded by NSERC
501 Discovery Grant (RGPIN-2020-03922). FR and VD are funded by CIHR (Team Grant: Canadian
502 Microbiome Initiative 2: Research Teams – Dissecting host-microbiome modifiers of type 2 diabetes risk
503 and complications). Computing was performed on Digital Research Alliance of Canada infrastructure (FR,
504 RRG2734). This work was also supported by the Sentinelle Nord program (Laval University) via its support
505 to the Joint International Research Unit - MicroMenu (VD), which is funded by the Sentinelle Nord
506 programme supported by the Apogée programme.

507 **Declaration of interests:** The authors declare none.

508 **References:**

509

510 Aigner, E., Feldman, A., & Datz, C. (2014). Obesity as an Emerging Risk Factor for Iron Deficiency.
511 *Nutrients*, 3587–3600. <https://doi.org/10.3390/nu6093587>.

512 Aktas, G., Alcelik, A., Yalcin, A., Karacay, S., Kurt, S., Akduman, M., & Savli, H. (2014). Treatment of
513 iron deficiency anemia induces weight loss and improves metabolic parameters. *Clin Ter.*
514 <https://doi.org/10.7471/CT.2014.1688>.

515 Al Bander, Z., Dekker Nitert, M., Mousa, A., & Naderpoor, N. (2020). The Gut Microbiota and
516 Inflammation: An Overview. *Int J Environ Res Public Health*, 20, 1–21.
517 <https://doi.org/10.3390/ijerph17207618>.

518 Alhouayek, M., & Muccioli, G. G. (2014). Harnessing the anti-inflammatory potential of
519 palmitoylethanolamide. *Drug Discov Today*, 19, 1632–1639. <https://doi.org/10.1016/j.drudis.2014.06.007>.

520 Almeida, M. M., Dias-Rocha, C. P., Calviño, C., & Trenzoli, I. H. (2022). Lipid endocannabinoids in
521 energy metabolism, stress and developmental programming. *Mol Cell Endocrinol*, 542.
522 <https://doi.org/10.1016/j.mce.2021.111522>.

523 Ananda Rao, G., Manix, M., & Larkin, E. C. (1980). Reduction of essential fatty acid deficiency in rat fed
524 a low iron fat free diet. *Lipids*, 15(1), 55–60. <https://doi.org/10.1007/BF02534119>.

525 Annuzzi, G., Piscitelli, F., Marino, L. Di, Patti, L., Giacco, R., Costabile, G., Bozzetto, L., Riccardi, G.,
526 Verde, R., Petrosino, S., Rivellese, A. A., & Marzo, V. Di. (2010). Differential alterations of the
527 concentrations of endocannabinoids and related lipids in the subcutaneous adipose tissue of obese diabetic
528 patients. *Lipids Health Dis*, 9, 1–8. <https://doi.org/10.1186/1476-511X-9-43>.

529 Asperti, M., Gryzik, M., Brilli, E., Castagna, A., Corbella, M., Gottardo, R., Girelli, D., Tarantino, G.,
530 Arosio, P., & Poli, M. (2018). Sucrosomial® Iron Supplementation in Mice: Effects on Blood Parameters,
531 Hepcidin, and Inflammation. *Nutrients*, 10(10), 1349. <https://doi.org/10.3390/nu10101349>

532 B R Blakley, D. L. H. (1988). The effect of iron deficiency on the immune response in mice. *Drug Nutr*
533 *Interact*, 5, 249-55.

534 Barrie, N., & Manolios, N. (2017). The endocannabinoid system in pain and inflammation: Its relevance to
535 rheumatic disease. *J Rheumatol*, 4, 210–218. <https://doi.org/10.5152/eurjrheum.2017.17025>.

536 Baumgartner, J., Smuts, C. M., Aeberli, I., Malan, L., Tjalsma, H., & Zimmermann, M. B. (2013).
537 Overweight impairs efficacy of iron supplementation in iron-deficient South African children: a
538 randomized controlled intervention. *IJO*, 24–30. <https://doi.org/10.1038/ijo.2012.145>.

539 Boulangé, C. L., Neves, A. L., Chilloux, J., Nicholson, J. K., & Dumas, M. E. (2016). Impact of the gut
540 microbiota on inflammation, obesity, and metabolic disease. *Genome Med*, 8, 1–12.
541 <https://doi.org/doi:10.1186/s13073-016-0303-2>.

542 Callahan, B. J., McMurdie, P. J., Rosen, M. J., Han, A. W., Johnson, A. J. A., & Holmes, S. P. (2016).
543 DADA2: High-resolution sample inference from Illumina amplicon data. *Nat. Methods*, 13, 581–583.
544 <https://doi.org/10.1038/nmeth.3869>.

- 545 Cani, P. D., Possemiers, S., Van De Wiele, T., Guiot, Y., Everard, A., Rottier, O., Geurts, L., Naslain, D.,
546 Neyrinck, A., Lambert, D. M., Muccioli, G. G., & Delzenne, N. M. (2009). Changes in gut microbiota
547 control inflammation in obese mice through a mechanism involving GLP-2-driven improvement of gut
548 permeability. *Gut*, 1091–1103. <https://doi.org/10.1136/gut.2008.165886>.
- 549 Castonguay-paradis, S., Lacroix, S., Rochefort, G., Parent, L., Perron, J., Martin, C., Lamarche, B.,
550 Raymond, F., flamand, nicolas, Di Marzo, V., & Veilleux, A. (2020). Dietary fatty acid intake and gut
551 microbiota determine circulating endocannabinoidome signaling beyond the effect of body fat. *Sci Rep*, 10,
552 1–11. <https://doi.org/10.1038/s41598-020-72861-3>.
- 553 Cepeda-Lopez, A. C., Aeberli, I., & Zimmermann, M. B. (2013). Does Obesity Increase Risk for Iron
554 Deficiency? A Review of the Literature and the Potential Mechanisms. *Int J Vitam Nutr Res.*, 80, 263–270.
555 <https://doi.org/10.1024/0300-9831/a000033>
- 556 Cerami, C. (2017). Iron Nutriture of the Fetus, Neonate, Infant, and Child. *Ann Nutr Metab*, 8–14.
557 <https://doi.org/10.1159/000481447>.
- 558 Chon, S. H., Yin, X. Z., Dixon, J. L., & Storch, J. (2007). Intestinal monoacylglycerol metabolism:
559 Developmental and nutritional regulation of monoacylglycerol lipase and monoacylglycerol
560 acyltransferase. *J Biol Chem*, 282, 33346–33357. <https://doi.org/10.1074/jbc.M706994200>.
- 561 Christie, S., Gary A Wittert, Hui Li, & Page, A. J. (2018). Involvement of TRPV1 Channels in Energy
562 Homeostasis. *Front Endocrinol*, 1, 420. <https://doi.org/10.3389/fendo.2018.00420>.
- 563 Collado, M. C., Rautava, S., Isolauri, E., & Salminen, S. (2015). Gut microbiota: A source of novel tools
564 to reduce the risk of human disease? *Pediatr Res*, 182–188. <https://doi.org/10.1038/pr.2014.173>.
- 565 Cooksey, R. C., Jones, D., Gabrielsen, S., Huang, J., Simcox, J. A., Luo, B., Soesanto, Y., Rienhoff, H.,
566 Abel, E. D., & McClain, D. A. (2010). Dietary iron restriction or iron chelation protects from diabetes and
567 loss of β -cell function in the obese (*ob/ob lep^{-/-}*) mouse. *Am J Physiol Endocrinol Metab*, 298(6), E1236.
568 <https://doi.org/10.1152/ajpendo.00022.2010>.
- 569 Cuddihy, H., Macnaughton, W. K., & Sharkey, K. A. (2022). Role of the Endocannabinoid System in the
570 Regulation of Intestinal Homeostasis. *Cell Mol Gastroenterol Hepatol*, 14, 947–963.
571 <https://doi.org/10.1016/j.jcmgh.2022.05.015>.
- 572 Cunnane, S. C., & McAdoo, K. R. (1987). Iron Intake Influences Essential Fatty Acid and Lipid
573 Composition of Rat Plasma and Erythrocytes. *J Nutr*, 117(9), 1514–1519.
574 <https://doi.org/10.1093/jn/117.9.1514>.
- 575 De Filippo, C., Costa, A., Becagli, M. V., Monroy, M. M., Provensi, G., & Passani, M. B. (2023). Gut
576 microbiota and oleoylethanolamide in the regulation of intestinal homeostasis. *Front. Endocrinol*, 14,
577 1135157. <https://doi.org/10.3389/fendo.2023.1135157>.
- 578 Di Marzo, V. (2018). New approaches and challenges to targeting the endocannabinoid system. *Nat Rev*
579 *Drug Discov*, 12, 623–639. <https://doi.org/10.1038/nrd.2018.115>.
- 580 Dostal, A., Chassard, C., Hilty, F. M., Zimmermann, M. B., Jaeggi, T., Rossi, S., & Lacroix, C. (2012).
581 Iron Depletion and Repletion with Ferrous Sulfate or Electrolytic Iron Modifies the Composition and
582 Metabolic Activity of the Gut Microbiota in Rats. *J. Nutr*, 271–277. <https://doi.org/10.3945/jn.111.148643>.

- 583 Dostal, A., Lacroix, C., Bircher, L., Pham, V. T., Follador, R., Zimmermann, M. B., & Chassard, C. (2015).
584 Iron Modulates Butyrate Production by a Child Gut Microbiota In Vitro. *MBio*, 6(6).
585 <https://doi.org/10.1128/mBio.01453-15>.
- 586 Ellulu, M. S., Patimah, I., Khaza'ai, H., Rahmat, A., & Abed, Y. (2017). Obesity and inflammation: the
587 linking mechanism and the complications. *Arch Med Sci*, 13(4), 851–863.
588 <https://doi.org/doi:10.5114/aoms.2016.58928>.
- 589 Everard, A., Plovier, H., Rastelli, M., Van Hul, M., De Wouters D'oplinter, A., Geurts, L., Druart, C.,
590 Robine, S., Delzenne, N. M., Muccioli, G. G., De Vos, W. M., Luquet, S., Flamand, N., Marzo, V. Di, &
591 Cani, P. D. (2019). Intestinal epithelial N-acylphosphatidylethanolamine phospholipase D links dietary fat
592 to metabolic adaptations in obesity and steatosis. *Nat Commun*, 1–17. [https://doi.org/10.1038/s41467-018-](https://doi.org/10.1038/s41467-018-08051-7)
593 [08051-7](https://doi.org/10.1038/s41467-018-08051-7).
- 594 Feng, Q., Wei-Dong Chen, & Yan-Dong Wang. (2018). Gut Microbiota: An Integral Moderator in Health
595 and Disease. *Front Microbiol*, 1–8. <https://doi.org/10.3389/fmicb.2018.00151>.
- 596 Gaetani, S., Fu, J., Cassano, T., Dipasquale, P., Romano, A., Righetti, L., Cianci, S., Laconca, L., Giannini,
597 E., Scaccianoce, S., Mairesse, J., Cuomo, V., & Piomelli, D. (2010). The Fat-Induced Satiety Factor
598 Oleoylethanolamide Suppresses Feeding through Central Release of Oxytocin. *J Neurosci*, 30(24), 8096.
599 <https://doi.org/10.1523/JNEUROSCI.0036-10.2010>.
- 600 Gaetani S, K. W. C. V. P. D. (2008). Role of endocannabinoids and their analogues in obesity and eating
601 disorders. *Eat Weight Disord*, 1, 1–8.
- 602 Gao, Y., Li, Z., Scott Gabrielsen, J., Simcox, J. A., Lee, S. H., Jones, D., Cooksey, B., Stoddard, G., Cefalu,
603 W. T., & McClain, D. A. (2015). Adipocyte iron regulates leptin and food intake. *J Clin Invest*, 125, 3681–
604 3691. <https://doi.org/10.1172/JCI181860>.
- 605 Grimaldi, P. A. (2001). The roles of PPARs in adipocyte differentiation. *Prog Lipid Res*, 40(4), 269–281.
606 [https://doi.org/10.1016/s0163-7827\(01\)00005-4](https://doi.org/10.1016/s0163-7827(01)00005-4).
- 607 Guevara Agudelo, F. A., Leblanc, N., Bourdeau-Julien, I., St-Arnaud, G., Lacroix, S., Martin, C., Flamand,
608 N., Veilleux, A., Di Marzo, V., & Raymond, F. (2022). Impact of selenium on the intestinal microbiome-
609 eCBome axis in the context of diet-related metabolic health in mice. *Front Immunol*, 13, 1–15.
610 <https://doi.org/10.3389/fimmu.2022.1028412>.
- 611 Hentze, M. W., Muckenthaler, M. U., & Andrews, N. C. (2004). Balancing Acts: Molecular Control of
612 Mammalian Iron Metabolism. *Cell*, 285–297. [https://doi.org/10.1016/s0092-8674\(04\)00343-5](https://doi.org/10.1016/s0092-8674(04)00343-5).
- 613 Hillard, C. J. (2017). Circulating Endocannabinoids: From Whence Do They Come and Where are They
614 Going? *NPP Reviews*, 43, 155–172. <https://doi.org/10.1038/npp.2017.130>.
- 615 Hisakawa, N., Nishiya, K., Tahara, K., Matsumori, A., & Hashimoto, K. (1998). Down regulation by iron
616 of prostaglandin E 2 production by human synovial fibroblasts. *Ann Rheum Dis*, 57, 742–746.
617 <https://doi.org/10.1136/ard.57.12.742>.
- 618 Iannotti, F. A., & Di Marzo, V. (2021). The gut microbiome, endocannabinoids and metabolic disorders. *J*
619 *Endocrinol*, 248(2), R83–R97. <https://doi.org/10.1530/JOE-20-0444>.
- 620 Ippolito, J. R., Piccolo, B. D., Robeson, M. S., Barney, D. E., Ali, J., Singh, P., & Hennigar, S. R. (2022).
621 Iron deficient diets modify the gut microbiome and reduce the severity of enteric infection in a mouse model

- 622 of S. Typhimurium-induced enterocolitis. *J Nutr Biochem*, 107.
623 <https://doi.org/10.1016/j.jnutbio.2022.109065>.
- 624 Johnson, S. B., Kramer, T. R., Briske-Anderson, M., & Holman, R. T. (1989). Fatty acid pattern of tissue
625 phospholipids in copper and iron deficiencies. *Lipids*, 24(2), 141–145.
626 <https://doi.org/10.1007/BF02535252>.
- 627 Kaitha, S., Bashir, M., & Ali, T. (2015). Iron deficiency anemia in inflammatory bowel disease. *World J*
628 *Gastrointest Pathophysiol*, 62. <https://doi.org/10.4291/wjgp.v6.i3.62>.
- 629 Kiela, P. R., & Ghishan, F. K. (2016). Physiology of Intestinal Absorption and Secretion. *Best Pract Res*
630 *Clin Gastroenterol*, 30, 145–159. <https://doi.org/10.1016/j.bpg.2016.02.007>.
- 631 Kitamura, N., Yokoyama, Y., Taoka, H., Nagano, U., Hosoda, S., Taworntawat, T., Nakamura, A., Ogawa,
632 Y., Tsubota, K., & Watanabe, M. (2021). Iron supplementation regulates the progression of high fat diet
633 induced obesity and hepatic steatosis via mitochondrial signaling pathways. *Sci Rep*, 11, 1–17.
634 <https://doi.org/10.1038/s41598-021-89673-8>.
- 635 Kortman, G. A. M., Raffatellu, M., Swinkels, D. W., & Tjalsma, H. (2014). Nutritional iron turned inside
636 out: intestinal stress from a gut microbial perspective. *FEMS Microbiol Rev*, 1202–1234.
637 <https://doi.org/10.1111/1574-6976.12086>.
- 638 Kostic, A. D., Xavier, R. J., & Gevers, D. (2014). The microbiome in inflammatory bowel disease: Current
639 status and the future ahead. *Gastroenterol*, 1489–1499. <https://doi.org/10.1053/j.gastro.2014.02.009>.
- 640 Lacroix, S., Pechereau, F., Leblanc, N., Boubertakh, B., Houde, A., Martin, C., Flamand, N., Silvestri, C.,
641 Raymond, F., Marzo, V. Di, Veilleux, A., & David, L. A. (2019). Rapid and Concomitant Gut Microbiota
642 and Endocannabinoidome Response to Diet-Induced Obesity in Mice. *MSystems*, 4, 1–14.
643 <https://doi.org/10.1128/mSystems.00407-19>.
- 644 Lakhali-Littleton, S., & Robbins, P. A. (2017). The interplay between iron and oxygen homeostasis with a
645 particular focus on the heart. *J Appl Physiol*, 967–973. <https://doi.org/10.1152/jappphysiol.00237.2017>.
- 646 Lê, S., Josse, J., & Husson, F. (2008). FactoMineR: An R Package for Multivariate Analysis. *J Stat Softw*,
647 25, 1–18. <https://doi.org/10.18637/jss.v025.i01>.
- 648 Livak, K. J., & Schmittgen, T. D. (2001). Analysis of Relative Gene Expression Data Using Real-Time
649 Quantitative PCR and the $2^{-\Delta\Delta CT}$ Method. *Methods*, 25, 402–408.
650 <https://doi.org/10.1006/meth.2001.1262>.
- 651 Lynch, S. R., & Cook, J. D. (1980). Interaction of Vitamin C and Iron. *Ann. N.Y. Acad. Sci*, 355(1), 32–
652 44. <https://doi.org/10.1111/j.1749-6632.1980.tb21325.x>.
- 653 Manca, C., Boubertakh, B., Leblanc, N., Deschênes, T., Lacroix, S., Martin, C., Houde, A., Veilleux, A.,
654 Flamand, N., Muccioli, G. G., Raymond, F., Cani, P. D., Di Marzo, V., & Silvestri, C. (2020). Germ-free
655 mice exhibit profound gut microbiota-dependent alterations of intestinal endocannabinoidome signaling. *J*
656 *Lipid Res*, 70–85. <https://doi.org/10.1194/jlr.RA119000424>.
- 657 Manios, Y., Moschonis, G., Chrousos, G. P., Lionis, C., Mougios, V., Kantilafi, M., Tzotzola, V., Skenderi,
658 K. P., Petridou, A., Tsalis, G., Sakellaropoulou, A., Skouli, G., & Katsarou, C. (2013). The double burden
659 of obesity and iron deficiency on children and adolescents in Greece: the Healthy Growth Study. *J Hum*
660 *Nutr Diet*, 26(5), 470–478. <https://doi.org/10.1111/jhn.12025>.

- 661 Matias, I., Gatta-Cherifi, B., Tabarin, A., Clark, S., Leste-Lasserre, T., Marsicano, G., Piazza, P. V., &
662 Cota, D. (2012). Endocannabinoids measurement in human saliva as potential biomarker of obesity. *PLoS*
663 *One*, 7(7), 1–9. <https://doi.org/10.1371/journal.pone.0042399>.
- 664 Mattera, R., Stone, G. P., Bahhur, N., & Kuryshev, Y. A. (2001). Increased release of arachidonic acid and
665 eicosanoids in iron-overloaded cardiomyocytes. *Circ*, 103, 2395–2401.
666 <https://doi.org/10.1161/01.cir.103.19.2395>.
- 667 McMurdie, P. J., & Holmes, S. (2014). Waste Not, Want Not: Why Rarefying Microbiome Data Is
668 Inadmissible. *PLoS Comput Biol*, 10, 1–12. <https://doi.org/10.1371/journal.pcbi.1003531>.
- 669 Moles, L., & Otaegui, D. (2020). The Impact of Diet on Microbiota Evolution and Human Health. Is Diet
670 an Adequate Tool for Microbiota Modulation? *Nutrients*, 1–30. <https://doi.org/doi:10.3390/nu12061654>.
- 671 Moore Heslin, A., O'donnell, A., Buffini, M., Nugent, A. P., Walton, J., Flynn, A., & McNulty, B. A.
672 (2021). Risk of iron overload in obesity and implications in metabolic health. *Nutrients*, 13(5), 1539.
673 <https://doi.org/10.3390/nu13051539>.
- 674 Müller, T. D., Finan, B., Bloom, S. R., D'Alessio, D., Drucker, D. J., Flatt, P. R., Fritsche, A., Gribble, F.,
675 Grill, H. J., Habener, J. F., Holst, J. J., Langhans, W., Meier, J. J., Nauck, M. A., Perez-Tilve, D., Pocai,
676 A., Reimann, F., Sandoval, D. A., Schwartz, T. W., ... Tschöp, M. H. (2019). Glucagon-like peptide 1
677 (GLP-1). *Mol Metab*, 30, 72–130. <https://doi.org/10.1016/j.molmet.2019.09.010>.
- 678 Nairz, M., Schroll, A., Sonnweber, T., & Weiss, G. (2010). The struggle for iron - a metal at the host-
679 pathogen interface. *Cell Microbiol*, 12, 1691–1702. <https://doi.org/10.1111/j.1462-5822.2010.01529.x>.
- 680 Nairz, M., & Weiss, G. (2020). Iron in infection and immunity. *Mol Asp Med*, 75, 1–18.
681 <https://doi.org/10.1016/j.mam.2020.100864>.
- 682 Ni, S., Yuan, Y., Kuang, Y., Li, X., Zhou, B., Di, A., & Scindia, Y. M. (2022). Iron Metabolism and Immune
683 Regulation. *Front. Immunol*, 1–11. <https://doi.org/10.3389/fimmu.2022.816282>.
- 684 Nutrition, N. R. C. (US) S. on L. A. (1995). *Nutrient Requirements of the Mouse*. National Academies
685 Press (US).
- 686 Oexle, H., Gnaiger, E., & Weiss, G. (1999). Iron-dependent changes in cellular energy metabolism:
687 Influence on citric acid cycle and oxidative phosphorylation. *BBA*, 99–107. [https://doi.org/10.1016/s0005-](https://doi.org/10.1016/s0005-2728(99)00088-2)
688 [2728\(99\)00088-2](https://doi.org/10.1016/s0005-2728(99)00088-2).
- 689 Okamoto, Y., Morishita, J., Tsuboi, K., Tonai, T., & Ueda, N. (2004). Molecular characterization of a
690 phospholipase D generating anandamide and its congeners. *J Biol Chem*, 279, 5298–5305.
691 <https://doi.org/10.1074/jbc.M306642200>.
- 692 Pereira, F. C., & Berry, D. (2017). Microbial nutrient niches in the gut. *Environ Microbiol*, 19, 1366–1378.
693 <https://doi.org/10.1111/1462-2920.13659>.
- 694 Peterson, D. A., Gerrard, J. M., Rao, G. H. R., Krick, T. P., & White, J. G. (1978). Ferrous iron mediated
695 oxidation of arachidonic acid: studies employing nitroblue tetrazolium (NBT). *Prostaglandins Med*, 1, 304–
696 317. [https://doi.org/10.1016/0161-4630\(78\)90050-2](https://doi.org/10.1016/0161-4630(78)90050-2).
- 697 Piomelli, D. (2013). A fatty gut feeling. *Trends Endocrinol Metab*, 24, 332–341.
698 <https://doi.org/10.1016/j.tem.2013.03.001>.

- 699 Piskin, E., Cianciosi, D., Gulec, S., Tomas, M., & Capanoglu, E. (2022). Iron Absorption: Factors,
700 Limitations, and Improvement Methods. *ACS Omega*, 7(24), 20441–20456.
701 <https://doi.org/10.1021/acsomega.2c01833>.
- 702 Poursharifi, P., Murthy, R., Prentki, M., & Murthy Madiraju, S. R. (2017). Monoacylglycerol signalling
703 and ABHD6 in health and disease. *Diabetes Obes Metab*, 1. <https://doi.org/10.1111/dom.13008>.
- 704 Psichas, A., Reimann, F., & Gribble, F. M. (2015). Gut chemosensing mechanisms. *JCI*, 125(3), 908.
705 <https://doi.org/10.1172/JCI76309>.
- 706 Rockfield, S., Chhabra, R., Robertson, M., Rehman, N., Bisht, R., & Nanjundan, M. (2018). Links Between
707 Iron and Lipids: Implications in Some Major Human Diseases. *Pharm*, 11.
708 <https://doi.org/10.3390/ph11040113>.
- 709 Rodríguez-Pérez, C., Vrhovnik, P., González-Alzaga, B., Fernández, M. F., Martín-Olmedo, P., Olea, N.,
710 Fiket, Ž., Kniewald, G., & Arrebola, J. P. (2018). Socio-demographic, lifestyle, and dietary determinants
711 of essential and possibly-essential trace element levels in adipose tissue from an adult cohort. *Environ*
712 *Pollut*, 878–888. <https://doi.org/10.1016/j.envpol.2017.09.093>.
- 713 Romano, A., Coccorello, R., Giacobazzo, G., Bedse, G., Moles, A., & Gaetani, S. (2014).
714 Oleoylethanolamide: A Novel Potential Pharmacological Alternative to Cannabinoid Antagonists for the
715 Control of Appetite. *Biomed Res Int*, 1–10. <https://doi.org/10.1155/2014/203425>.
- 716 Romero, A. M., Jordá, T., Rozès, N., Martínez-Pastor, M. T., & Puig, S. (2018). Regulation of yeast fatty
717 acid desaturase in response to iron deficiency. *Biochim Biophys Acta Mol Cell Biol Lipids*, 1863(6), 657–
718 668. <https://doi.org/10.1016/j.bbalip.2018.03.008>.
- 719 Rowland, I., Gibson, G., Heinken, A., Scott, K., Swann, J., Thiele, I., Tuohy, K., Heinken Almutheinken,
720 A., Karen Scott KScott, unilu, & Jonathan Swann, abdnacuk. (2018). Gut microbiota functions: metabolism
721 of nutrients and other food components. *Eur J Nutr*, 1–24. <https://doi.org/10.1007/s00394-017-1445-8>.
- 722 Santos, M., Clevers, H., De Sousa, M., & Marx, J. J. M. (1998). Adaptive Response of Iron Absorption to
723 Anemia, Increased Erythropoiesis, Iron Deficiency, and Iron Loading in β 2-Microglobulin Knockout Mice.
724 *Blood*, 91(8), 3059–3065. <https://doi.org/10.1182>
- 725 Seltzer, C. C., & Mayer, J. (1963). Serum iron and iron-binding capacity in adolescents. ii. comparison of
726 obese and nonobese subjects. *Am J Clin Nutr*, 13, 354–361. <https://doi.org/10.1093/ajcn/13.6.354>.
- 727 Seyoum, Y., Baye, K., & Humblot, C. (2021). Iron homeostasis in host and gut bacteria – a complex
728 interrelationship. *Gut Microbes*, 13. <https://doi.org/10.1080/19490976.2021.1874855>.
- 729 Silvestri, C., & Di Marzo, V. (2013). The endocannabinoid system in energy homeostasis and the
730 etiopathology of metabolic disorders. *Cell Metab*, 17(4), 475–490.
731 <https://doi.org/doi:10.1016/j.cmet.2013.03.001>.
- 732 Simard, M., Archambault, A. S., Lavoie, J. P. C., Dumais, É., Di Marzo, V., & Flamand, N. (2022).
733 Biosynthesis and metabolism of endocannabinoids and their congeners from the monoacylglycerol and N-
734 acyl-ethanolamine families. *Biochem Pharmacol*, 205, 115261.
735 <https://doi.org/doi:10.1016/j.bcp.2022.115261>.
- 736 Sung, Y., Yu, Y. C., & Han, J. M. (2023). Nutrient sensors and their crosstalk. *Exp Mol Med*, 55(6), 1076–
737 1089. <https://doi.org/10.1038/s12276-023-01006-z>.

- 738 Taschler, U., Hasenoehrl, C., Storr, M., & Schicho, R. (2017). Cannabinoid Receptors in Regulating the GI
739 Tract: Experimental Evidence and Therapeutic Relevance. *Handb Exp Pharmacol*, 239, 343–362.
740 https://doi.org/10.1007/164_2016_105.
- 741 Turcotte, C., Archambault, A.-S., Dumais, É., Martin, C., Blanchet, M.-R., Bissonnette, E., Ohashi, N.,
742 Yamamoto, K., Laviolette, M., Veilleux, A., Boulet, | Louis-Philippe, Marzo, V. Di, & Flamand, N. (2020).
743 Endocannabinoid hydrolysis inhibition unmasks that unsaturated fatty acids induce a robust biosynthesis
744 of 2-arachidonoyl-glycerol and its congeners in human myeloid leukocytes. *FASEB J*, 4253–4265.
745 <https://doi.org/10.1096/fj.201902916R>.
- 746 V M Showalter, D. R. C. B. R. M. M. E. A. (1996). Evaluation of binding in a transfected cell line
747 expressing a peripheral cannabinoid receptor (CB2): identification of cannabinoid receptor subtype
748 selective ligands. *J Pharmacol Exp Ther*, 3, 989–999.
- 749 Viaud, S., Daillère, R., Boneca, I. G., Lepage, P., Pittet, M. J., Ghiringhelli, F., Trinchieri, G., Goldszmid,
750 R., & Zitvoige, L. (2014). Harnessing the intestinal microbiome for optimal therapeutic immunomodulation.
751 *Cancer Res*, 4217–4221. <https://doi.org/10.1158/0008-5472.CAN-14-0987>.
- 752 Wenzel, B. J., Stults, H. B., & Mayer, J. (1962). Hypoferraemia in obese adolescents. *Lancet*, 280, 327–
753 328. [https://doi.org/10.1016/s0140-6736\(62\)90110-1](https://doi.org/10.1016/s0140-6736(62)90110-1).
- 754 Wright, M. O., & Fischer, J. G. (1997). The Effect of High Dietary Iron and Low Vitamin E on Lipid
755 Peroxidation and Prostaglandin E2 in a Model of Colon Cancer. *J Am Diet Assoc*, 97.
756 [https://doi.org/10.1016/S0002-8223\(97\)00540-3](https://doi.org/10.1016/S0002-8223(97)00540-3).
- 757 Yanoff, L. B., Menzie, C. M., Denkinger, B., Sebring, N. G., McHugh, T., Remaley, A. T., & Yanovski, J.
758 A. (2007). Inflammation and iron deficiency in the hypoferremia of obesity. *IJO*, 31, 1412–1419.
759 <https://doi.org/10.1038/sj.ijo.0803625>.
- 760 Yilmaz, B., & Li, H. (2018). Gut Microbiota and Iron: The Crucial Actors in Health and Disease. *Pharm*,
761 11, 1–20. <https://doi.org/10.3390/ph11040098>.
- 762 Zhou, Y. E., Kubow, S., & Egeland, G. M. (2011). Is iron status associated with highly unsaturated fatty
763 acid status among Canadian Arctic Inuit? *Food Funct*, 2, 381–385. <https://doi.org/10.1039/C1FO10051C>
- 764